Nuclear Inst. and Methods in Physics Research B 429 (2018) 19–26

Contents lists available at ScienceDirect

Nuclear Inst. and Methods in Physics Research B

journal homepage: www.elsevier.com/locate/nimb

# Measurement of $L$ XRF cross sections for elements with $33 \le Z \le 51$ and their interpretation in terms of $L_i$ ($i$ = 1–3) subshell vacancy decay parameters

Heena Duggal[a], Veena Sharma[a,c,*], H.S. Kainth[a], Sanjeev Kumar[a,b], J.S. Shahi[a], D. Mehta[a]

[a] Department of Physics, Panjab University, Chandigarh 160014, India
[b] Department of Physics, G.G.D.S.D. College, Chandigarh 160030, India
[c] Department of Applied Physics, G.Z.S. College of Engineering and Technology, Bathinda 151001, India

ARTICLE INFO

*Keywords:*
X-ray fluorescence
Inner-shell vacancy decay
Fluorescence yield
Coster-Kronig yield

ABSTRACT

The $L_i$ ($i$ = 1–3) subshell integral X-ray fluorescence (XRF) cross sections have been measured for 17 elements with $33 \le Z \le 51$ following photoionization by the Mn $K$ X-rays ($E_{K\alpha\beta}$ = 5.96 keV). The $L_i$ ($i$ = 1–3) subshell X-rays were measured using a low-energy Ge (LEGe) detector at an emission angle, $\psi = 125°$, where angle-dependent emission effects, if any, are nullified as $P_2(\cos\psi) \sim 0$. The XRF cross sections were interpreted in terms of available sets of theoretical $L_i$ ($i$ = 1–3) subshell photoionization cross sections, radiative transition probabilities, and the atomic vacancy decay parameters, namely, fluorescence ($\omega_i$) and Coster-Kronig ($f_{ij}$) yields. A set of $L_1$ subshell fluorescence ($\omega_1$) yields was deduced for the elements with $37 \le Z \le 51$ from the present measured $L\gamma_{2,3,(4)}$ [$L_1$-$N_{2,3}(O_{2,3})$] XRF cross sections. The $\omega_1$ values exhibit jumps at $Z$ = 40 and 49, which are identified to be due to cut-off of the $L_1L_2M_{4,5}$ and $L_1L_3M_{4,5}$ Coster-Kronig (CK) transitions predicted by calculations based on relativistic Dirac-Hartree-Slater (RDHS) model. However, the measured $\omega_1$ values are found to differ considerably from those based on the RDHS model calculations for the elements below $Z$ = 50. The pronounced discrepancies between measured and theoretical $\omega_1$ values are likely to be due to overestimation of the $L_1$-$L_{2,3}M_{4,5}$ CK transition rates by a factor of ~2–3. Our experiential results demand consideration of extra-atomic relaxation from the solid-state effects and exchange splitting in many-body theoretical calculations of the low-energy CK transitions.

## 1. Introduction

The $L_i$ ($i$ = 1–3) subshell vacancies relax through the inter-shell hole transfer leading to emission of characteristic X-rays and Auger transitions, and the intra-shell hole transfer resulting in Coster-Kronig (CK) transitions. The set of fluorescence ($\omega_i$) and CK ($f_{ij}$) yields based on the relativistic Dirac-Hartree-Slater (RDHS) model are given by Chen et al. [1] for 25 elements with $18 \le Z \le 100$. Campbell [2] has critically examined all the available experimental and theoretical data related to the $L_i$ ($i$ = 1–3) subshell fluorescence and CK yields, and recommended a set of $\omega_i$ and $f_{ij}$ yields. Campbell [2] also pointed out paucity of experimental data for the $L_i$ subshells in the atomic region below Z ~ 60. Another data set of the $\omega_i$ and $f_{ij}$ yields that still bears relevance is the one based on Krause's semi-empirical fits [3] derived from the available experimental data till 1979. The $\omega_i$ and $f_{ij}$ parameters can be deduced by measuring the $L_i$ subshell X-rays at various photon energies across the $L_i$ ($i$ = 1–3) subshell binding energies. The accurate $L_i$ ($i$ = 1–3) subshell X-ray fluorescence (XRF) cross section data can infer regarding reliability of the atomic vacancy decay parameters. Refinements in the $L_i$ ($i$ = 1–3) subshell fluorescence and CK yields are justified by their important role in interpretation of the experiments that attempt to measure the inner-shell ionization cross sections of electrons, light ions ($p$,$\alpha$) and the number of initial primary vacancies in atomic subshells following the radioactive electron capture decay and internal conversion processes. The elemental analyses for the medium- and high-Z elements using wavelength-dispersive (WD) and the energy-dispersive (ED) X-ray fluorescence (XRF) setup are based on the $L_i$-subshell X-ray measurements and involve XRF cross sections calculated using the atomic vacancy decay parameters, $\omega_i$ and $f_{ij}$ yields.

The previous experimental data on L-shell X-ray studies are available for the rare-earth and higher-Z elements. The data regarding investigation of medium-Z elements are scarce due to the difficulties associated with the low-energy L X-ray measurements. Most of the available measurements [4,5] are related to the total L XRF cross

* Corresponding author at: Department of Applied Physics, G.Z.S. College of Engineering and Technology, Bathinda 151001, India.
*E-mail address:* vn.veena@gmail.com (V. Sharma).

https://doi.org/10.1016/j.nimb.2018.05.013
Received 20 February 2018; Received in revised form 6 May 2018; Accepted 10 May 2018

sections for the elements with $Z \sim$ 40–50 at the 5.96 keV photon energy using $^{55}$Fe radioactive source. Total L X-ray fluorescence cross sections have also been measured by Rao et al. [6] for the elements with $46 \leq Z \leq 51$ at the 6.47, 7.57 and 8.12 keV photon energies using quasi-monoenergetic excitation beam obtained from the Fe, Ni and Cu secondary exciters used in conjunction with the X-ray tube. The incident beam contains the characteristic K X-rays as well as bremsstrahlung photons scattered from the secondary exciters [7] and these measurements [6] lack proper quality corrections for the target excitation by the scattered photons. Han et al. [8] reported the $L\alpha$, $L\beta$ and total $L$ XRF cross sections for $_{40}$Zr, $_{41}$Nb, $_{42}$Mo, $_{47}$Ag, $_{48}$Cd, $_{49}$In, $_{50}$Sn, $_{51}$Sb and $_{53}$I at the 5.96 keV photon energy and reported deviations up to ~15% from the cross sections calculated using the $\omega_i$ and $f_{ij}$ values from the semi-empirical data set of Krause [3]. In the recent years, the $Ll$, $L\alpha$, $L\beta_{1,4,3,6}$, $L\beta_{2,15}$, $L\gamma_1$ and $L\gamma_{2,3,(4)}$ XRF cross sections for elements with $45 \leq Z \leq 50$ have been measured at the 8, 9 and 10 keV photon energies using monochromatized synchrotron sources [9–11]. The measured cross section for the $L\alpha$ and $L\beta_{1,4,3,6}$ X-rays agree with the ones calculated using Krause's $\omega_i$ and $f_{ij}$ values [3] while those for the $Ll$, $L\beta_{2,15}$, $L\gamma_1$ and $L\gamma_{2,3,(4)}$ X-rays exhibit considerable inconsistencies.

The present work reports XRF cross section measurements for various $L_i$ ($i$ = 1–3) subshell X-ray components/groups in 17 elements with $33 \leq Z \leq 51$ at the Mn $K\alpha\beta$ X-ray energy using energy dispersive detection set up. The measured results are interpreted in terms of the $L_i$ subshell photoionization cross sections, the X-ray emission rates and the atomic vacancy decay parameters ($\omega_i$ and $f_{ij}$ yields), which elucidates reliability of the available data sets of these parameters.

## 2. Experimental measurements

The $L_i$ (i = 1–3) subshell XRF cross section measurements were carried out using the source, target and detector geometrical arrangement shown in Fig. 1. The $^{55}$Fe annular exciter source [1.850 GBq, $T_{1/2}$ = 2.73 y, model IEC.A2, AEA Technology, Germany] is in the form of a circular flat ribbon of 34-mm diameter and 4-mm width. It undergoes electron capture decay resulting in the Mn K X-rays ($E_{K\alpha_2}$ = 5.888 keV, $E_{K\alpha_1}$ = 5.899 keV and $E_{K\beta_1}$ = 6.492 keV) with emission probabilities 8.2, 16.2 and 2.86 per 100 decays [12], respectively. The Mn K X-rays have been used to produce $L_i$ ($i$ = 1–3) subshell vacancies in the elements with $33 \leq Z \leq 51$. The weighted average energy of the Mn $K$ X-rays can be safely taken to be 5.96 keV after correcting for absorption in the source and its Al window. A low energy Ge (LEGe) detector (100 mm$^2$ × 10 mm, 8-μm Be window, energy resolution of ~150 eV at Mn $K\alpha$ X-ray energy, Canberra, US) was used to detect X-rays emitted from the target. The X-ray spectra were registered using multichannel analyzer (Multiport II, Canberra, US). The measurements were done under vacuum (~$10^{-2}$ torr) to avoid attenuation and scattering in air, and eliminate the $K$ X-ray ($E_{K\alpha\beta}$ = 2.975 keV) peaks due to $_{18}$Ar present in air. The detection efficiency of the present geometrical set up was optimized by adjusting the distance between target and detector so that

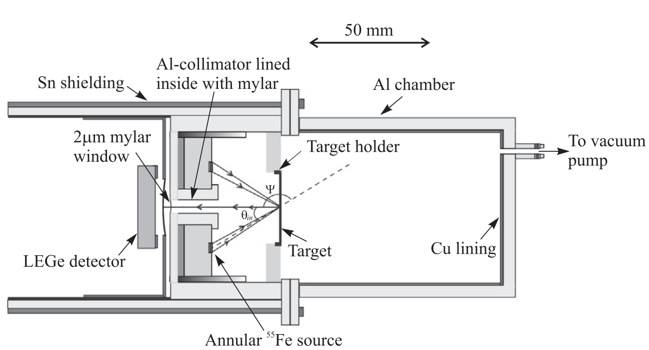


**Fig. 1.** Schematic arrangement of the present experimental set up (figure is to the scale) involving $^{55}$Fe annular source, target and LEGe detector.

the count rate of the X-rays coming from the target is maximum. The count rate is observed to remain constant within ± 1% over a distance of ~3 mm. The effective incident angle ($\theta_i = 180^\circ - \psi$) between the incident beam and the normal to the target surface was determined to be 125° using an *in-situ* method based on attenuation of the Mn $K\alpha$ X-rays [13].

The $L$ X-ray fluorescence measurements were performed using spectroscopically pure targets of Se (104 and 105 μg/cm$^2$), $SrF_2$ (55, 170 and 241 μg/cm$^2$), $YF_3$ (95 and 168 μg/cm$^2$), $Nb_2O_5$ (101 and 250 μg/cm$^2$), $MoO_3$ (105 and 189 μg/cm$^2$), Rh (152 μg/cm$^2$), Pd (157 and 206 μg/cm$^2$), Ag (47, 263 and 371 μg/cm$^2$), CdSe (152 and 356 μg/cm$^2$), In (100, 155 and 367 μg/cm$^2$), Sn (100, 186 and 372 μg/cm$^2$) and Sb (202 and 363 μg/cm$^2$) evaporated on the Mylar backing. These thin targets were procured from Micromatter, Deer Harbor, WA, US. Thick targets of the Y, Zr, Nb, Mo, Ru, Rh, Pd, Ag, Cd, In, Sn and Sb elements in the form of metallic foils (thickness ~10–70 mg/cm$^2$), and the As, Se, Br, Rb and Sr elements in the form of pellets of As, Se, NaBr, $RbNO_3$ and $SrCO_3$ powders were also used in the measurements. In order to reduce statistical error in the measured cross sections, three spectra of each target were taken for time duration ranging 5–15 h. In the observed spectra, the $L_i$ subshells X-ray peaks are well separated from the elastic and inelastic scatter Mn $K\alpha$ and $K\beta$ X-ray peaks and no interfering target impurity was noticed. The background spectra taken without target in the same geometrical set up were also found to be uncontaminated in the energy region of interest. The effective efficiency (intrinsic efficiency including the geometry factor) of the LEGe detector in the energy region 1.2–5.0 keV was determined by measuring the $K$ X-ray yield from thick targets of Mg, Al, Si, P, S, NaCl, $KBH_4$, $CaCO_3$, Ti and V, and thin targets of Al (158 and 161 μg/cm$^2$), SiO (95 and 229 μg/cm$^2$), GaP (234 μg/cm$^2$), CuS (194 and 91.3 μg/cm$^2$), NaCl (46.5 and 48.7 μg/cm$^2$), KCl (44.3 μg/cm$^2$), $CaF_2$ (69 and 133 μg/cm$^2$), $ScF_3$ (104 and 199 μg/cm$^2$), Ti (78 and 112 μg/cm$^2$) and V (100.4 and 203 μg/cm$^2$) evaporated onto 3.5 μm thick Mylar backing. These spectra were taken in the same evacuated geometrical set up as used for the actual fluorescent $L$ X-ray measurements. The spectra for the $CaF_2$ and V targets were taken at regular intervals to correct for decay of the $^{55}$Fe source during the measurements.

## 3. Evaluation procedure

### 3.1. Experimental XRF cross sections

The experimental differential cross sections for the $L_p$ group of the fluorescent X-rays in the elements with $33 \leq Z \leq 51$ at the 5.96 keV excitation energy have been evaluated using the expression

$$\frac{d\sigma_{LXp}}{d\Omega} = \frac{N_{Lp}}{m_u \beta_{Lp} (I_o G)_{K\alpha\beta} \varepsilon_{Lp}} \tag{1}$$

where $N_{Lp}$ is the number of counts per unit time under the photopeaks corresponding to the $Lp$ X-rays, $(I_o G)_{K\alpha\beta}$ factor is the effective intensity of the exciting Mn $K\alpha\beta$ X-rays falling on area of the target visible to the detector, $\varepsilon_{Lp}$ is the detector efficiency at the $Lp$ X-ray energy, and m is the mass thickness of target in g/cm$^2$. In case of compound target, $m$ is replaced by $m_u$ which represents mass-thickness of the $u$th element of interest in the target in g/cm$^2$. $\beta_{Lp}$ is the correction factor that accounts for attenuation of the incident Mn $K$ X-rays and the emitted $Lp$ X-rays in the target. The formulation to evaluate the $\beta_{Lp}$ values have been discussed elsewhere [13]. The values of $\beta_{Lp}$ are ≥0.90 for thin targets with mylar backing. In case of thick foil and pellet targets with $\beta_{Lp} < 0.21$, the limiting values of the effective thickness, $m_u\beta_{Lp}$, parameter calculated using Eq. (3) of Ref. [13] have been used. The L X-ray measurements were performed at an emission angle, $\psi = 125^\circ$, where the second-order Legendre polynomial term $P_2(\cos\psi)$ associated with the angular distribution of X-ray emission is nearly zero [14]. Integral cross sections were evaluated by multiplying the differential cross sections by